Research Article

Hydrogen Sulfide Suppresses Skin Fibroblast Proliferation *via* Oxidative Stress Alleviation and Necroptosis Inhibition

Ling Li [ID],[1,2] Ziying He [ID],[1] Yue Zhu [ID],[1] Qiyan Shen [ID],[1] Shengju Yang [ID],[1] and Shuanglin Cao [ID][1]

[1]*Department of Dermatology, Affiliated Hospital of Nantong University, Nantong 226001, China*
[2]*Yancheng No.1 People's Hospital, Yancheng 224001, China*

Correspondence should be addressed to Shengju Yang; yangshengju@ntu.edu.cn and Shuanglin Cao; caoshuanglin@ntu.edu.cn

Keloid is a common dermatofibrotic disease with excessive skin fibroblast proliferation. Hydrogen sulfide (H_2S) as the third gasotransmitter improves fibrosis of various organs and tissues. Our study is aimed at investigating the effects and possible mechanisms of H_2S on skin fibroblast proliferation. Scar tissues from six patients with keloid and discarded skin tissue from six normal control patients were collected after surgery, respectively. Plasma H_2S content and skin H_2S production in patients with keloid were measured. Keloid fibroblasts and transforming growth factor-β_1- (TGF-β_1, 10 ng/mL) stimulated normal skin fibroblasts were pretreated with H_2S donor as NaHS (50 μM) for 4 h. Cell migration after scratch was assessed. The expressions of α-smooth muscle actin (α-SMA), proliferating cell nuclear antigen (PCNA), collagen I, and collagen III were detected by immunofluorescence, real-time PCR, and/or Western blot. Intracellular superoxide anion and mitochondrial superoxide were evaluated by dihydroethidium (DHE) and MitoSOX staining, respectively. Mitochondrial membrane potential was detected by JC-1 staining. Apoptotic cells were detected by TDT-mediated dUTP nick end labeling (TUNEL). The expressions of receptor interacting protein kinase 1 (RIPK1), RIPK3, and mixed lineage kinase domain-like protein (MLKL) were measured by Western blot. We found that H_2S production was impaired in both the plasma and skin of patients with keloid. In keloid fibroblasts and TGF-β_1-stimulated normal skin fibroblasts, exogenous H_2S supplementation suppressed the expressions of α-SMA, PCNA, collagen I, and collagen III, reduced intracellular superoxide anion and mitochondrial superoxide, improved the mitochondrial membrane potential, decreased the positive rate of TUNEL staining, and inhibited RIPK1 and RIPK3 expression as well as MLKL phosphorylation. Overall, H_2S suppressed skin fibroblast proliferation *via* oxidative stress alleviation and necroptosis inhibition.

1. Introduction

Keloid is a common dermatofibrotic disease with main characteristics of excessive skin fibroblast proliferation and extracellular matrix accumulation [1]. Keloid is usually regarded as a benign skin tumor according to clinical manifestation, gene phenotype, pathological features, and prognosis [2]. Keloid has become a cosmetic problem because most protruding scar tissues are beyond the epidermis with obvious pigmentation. In addition, patients suffering from keloid usually feel pruritus and pain, which even cause psychological problems such as inferiority and anxiety [3].

Keloid can be treated by corticosteroid injection, radiotherapy, cryotherapy, 5-fluorouracil, tamponade, laser, and surgery [4]. However, there is still a high recurrence rate because of the lack of "gold standard" for keloid treatment [5]. Therefore, seeking effective interventions for keloid is a hot topic in clinic.

Transforming growth factor-β_1 (TGF-β_1) is recognized as one of the most important factors for fibrosis [6]. Previous studies have confirmed that the content of TGF-β_1 in keloid was significantly increased, while TGF-β_1 inhibition prevented keloid fibroblast proliferation and attenuated extracellular matrix synthesis [7]. However, TGF-β_1 blockage is

prone to causing extensive damage by diversified biological effects due to nonspecific inhibition. It is necessary to explore novel strategies to suppress keloid fibroblast proliferation and improve dermatofibrotic diseases.

Hydrogen sulfide (H_2S) is the third gasotransmitter with multiple functions, which plays a vital role in a variety of physiological and pathological processes [8]. H_2S is mainly generated by catalysis of cystathionine γ-lyase (CSE) in skin [9, 10]. Previous researches showed that H_2S promoted skin wound healing by inflammation inhibition, oxidative stress suppressing, and vascular endothelial growth factor (VEGF) enhancement [11–14]. H_2S supplement significantly alleviated skin pruritus in mice [15]. H_2S also induced apoptosis and blocked the activation of nuclear factors-κB (NF-κB) to inhibit melanoma cells growth and prevent tumor progression [16, 17]. That is to say, H_2S showed protective effects against various skin diseases. Additionally, previous studies found that H_2S inhibited the activation of fibrosis-related cells and cytokine expression, then alleviated renal fibrosis, and improved renal function in the rats with renal sclerosis caused by renal tubular epithelial mesenchymal transition (EMT) [18]. Exogenous H_2S significantly decreased the level of TGF-β_1 *in vivo*, increased the expression of aortic elastin, and prevented diabetic nephropathy arteriosclerosis in rats [19]. H_2S improved myocardial fibrosis *via* suppressing the TGF-β_1/Smad signaling pathway [20]. H_2S inhibited the TGF-β_1/Smad signaling pathway, improved lung function, and alleviated dermatitis, pulmonary alveoli injury, and chronic obstructive pulmonary fibrosis in cigarette smoke-induced chronic obstructive pulmonary disease of rats [21, 22]. The evidence demonstrated that H_2S had potential effects on fibrotic diseases [23]. However, the possible effect of H_2S on keloid and other dermatofibrotic disease remains unknown. A recent study showed that the impairment of endogenous H_2S aggravated mitochondrial damage, increased reactive oxygen species (ROS), and induced necroptosis to aggravate diabetic cardiomyopathy. Exogenous H_2S improved mitochondrial function, inhibited oxidative stress, and reduced necroptosis to improve diabetic cardiomyopathy [24]. Moreover, H_2S donors inhibited necroptosis and alleviated hypoxia-induced myocardial fibroblast proliferation depending on sirtuin 3 [25]. However, whether oxidative stress and necroptosis were involved in the possible effect of H_2S on skin fibroblast proliferation has not been known well.

Therefore, NaHS, a common H_2S donor, was applied to investigate whether exogenous H_2S supplementation could reverse excessive proliferation in keloid fibroblasts and in TGF-β_1-induced normal skin fibroblasts. In addition, the mechanisms of H_2S on skin fibroblast proliferation were further explored from the perspective of oxidative stress and necroptosis. It is beneficial to provide a novel strategy for the prevention and treatment of dermatofibrotic diseases including keloid, which has a potential clinical transformation prospect.

2. Materials and Methods

2.1. Collection of Human Skin Samples.
Scar tissues from six patients with keloid and discarded skin tissue from six nor-mal control patients without any skin diseases were collected after surgery, respectively. All cases of keloid and normal control were free of infection, tumor, cardiovascular diseases, renal diseases, diabetes mellitus, and other systemic diseases. All patients were not subjected to any local drug injection, radiation, or surgical treatment within the latest 2 years, and any topical drug treatment within the latest 1 month. Plasma was also collected from the above patients. The study strictly followed the requirements of the Declaration of Helsinki. All patients signed a written informed consent. The research was approved by the ethics committee of Affiliated Hospital of Nantong University (No. 2020-L146).

2.2. Determination of H_2S Levels in Plasma and Skin.
After polarization, H_2S-specific microelectrode was inserted into the plasma. The current change was measured by the connected free radical analyzer (World Precision Instruments Inc., Sarasota, Florida, USA). H_2S concentration was calculated according to the standard curve drawn by the standard concentration and corresponding currents. The concentration of H_2S in plasma was calibrated with that in normal control.

The collected skin samples were cut into pieces and homogenized (1/10, w/v) in K_2PO_4 (100 mM). Then 460 μL homogenization buffer was taken, and 20 μL L-cysteine (10 mM) and 20 μL pyridoxal-5$'$-phosphate (2 mM) were sequentially added. The H_2S level was measured as the above methods. H_2S production in the skin was calculated according to the standard curve and normalized with protein concentration, which were calibrated with that in normal control.

2.3. Primary Skin Fibroblasts Culture and Treatment.
After removing epidermis and surrounding fat, skin samples were cut into pieces of 1 mm^3, cultured in Dulbecco's modified Eagle's medium (DMEM, Gibco, Grand Island, New York, USA) with 10% fetal bovine serum (FBS, Gibco, Grand Island, New York, USA) and subcultured for further experiments. Keloid fibroblasts from keloid were pretreated with NaHS (50 μM, Sigma-Aldrich, St. Louis, MO) for 4 h. Skin fibroblasts from normal skin were pretreated with NaHS (50 μM) for 4 h followed with or without TGF-β_1 (10 ng/ml, PeproTech, Suzhou, China) stimulation for 12 h. The same amount of culture medium was given as a control group.

2.4. Cell Migration Assay after Scratch.
After the above treatment, skin fibroblasts were scratched with pipette tips of 10 μL, and the shedding cells were washed out with PBS. Cell migration was recorded by photograph after scratch for 0, 4, 8, 12, and 24 h. The migration rate of cells was calculated as the ratio of the migrated area to the original area.

2.5. Immunofluorescent Staining.
After incubation with α-smooth muscle actin (α-SMA, 1 : 100; Bosterbio, Wuhan, China), proliferating cell nuclear antigen (PCNA, 1 : 100; Abclonal, Wuhan, China), and collagen I and collagen III (1 : 100; Bosterbio, Wuhan, China) antibodies overnight at 4°C, skin fibroblasts were incubated with Cy3- or Alexa Fluor 488-conjugated IgG (1 : 500; Beyotime, Shanghai, China) for 2 h in the dark. Nuclei were stained by 4$'$,6-
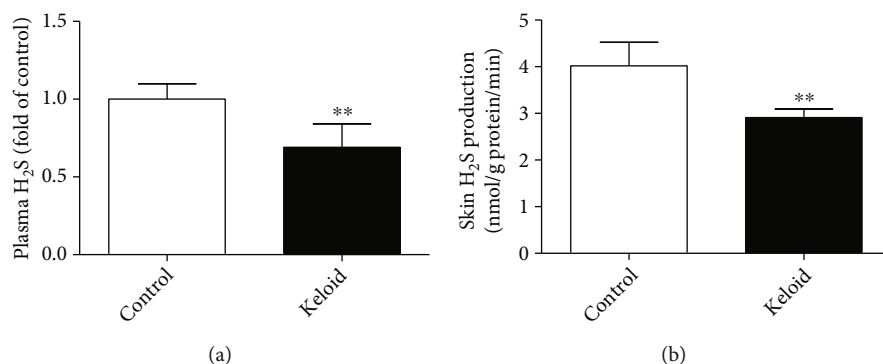
(a)

(b)

FIGURE 1: H_2S production was impaired in patients with keloid. Scar tissues from patients with keloid (Keloid) and discarded skin tissue from normal control patients (Control) were collected after surgery, respectively. Plasma was also collected from above patients. (a) Plasma H_2S content was detected. (b) Skin H_2S production was assessed. $^{**}P < 0.01$ vs. control, $n = 6$.
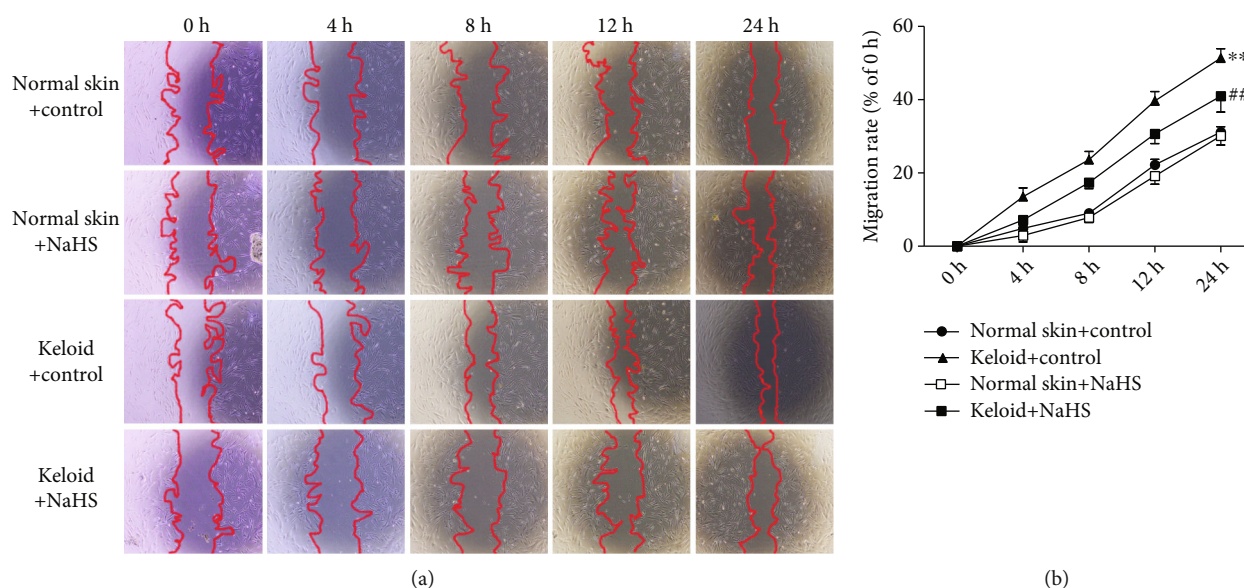

(a)

(b)

FIGURE 2: NaHS inhibited keloid fibroblast migration after scratch. Skin fibroblasts were extracted from skin tissues of normal controls (normal skin) and scar tissue from patients with keloid (keloid), respectively. After pretreatment with NaHS ($50\,\mu$M) or the same amount of culture medium (control) for 4 h, the fresh culture medium was replaced. The cells were scratched with a $10\,\mu$L pipette tip 12 h later. (a) Photos were taken after scratch for 0 h, 4 h, 8 h, 12 h, and 24 h. (b) The percentage of cell migration area to initial scratch area at different time. $^{**}P < 0.01$ vs. normal skin + control; $^{\#\#}P < 0.01$ vs. keloid + control, $n = 6$.

diamidino-2-phenylindole (DAPI, Beyotime, Shanghai, China). The fluorescence was observed and photographed with a laser confocal microscope (Leica, Wetzlar, Germany). The fluorescence intensity was evaluated with the ImageJ software and expressed as the fold of that in control group.

2.6. Dihydroethidium (DHE) Staining. After incubation with DHE ($2\,\mu$M, Beyotime, Shanghai, China) at 37°C for 30 min in the dark, the superoxide anion production in skin fibroblasts was evaluated as DHE fluorescence intensity which were observed and photographed with a laser confocal microscope.

2.7. Mitochondrial Superoxide Detection. Mitochondrial superoxide in skin fibroblasts was detected with MitoSOX ($5\,\mu$M, YEASEN, Shanghai, China) staining. MitoTracker Green (200 nM, Beyotime, Shanghai, China) was incubated

for mitochondria colocation at 37°C for 20 min in the dark. The fluorescence was observed and photographed with a laser confocal microscope.

2.8. Mitochondrial Membrane Potential ($\Delta\psi m$) Detection. After incubation with JC-1 staining solution (Beyotime, Shanghai, China) at 37°C for 20 min in the dark, the fluorescence in skin fibroblasts was observed with a laser confocal microscope at 495/519 nm wavelengths for JC-1 Monomers and 550/570 nm wavelengths for JC-1 Aggregates, respectively.

2.9. TdT-Mediated dUTP Nick End Labeling (TUNEL) Staining. After incubation with PBS containing 0.5% Triton X-100 at room temperature for 5 min, the skin fibroblasts were incubated with the TUNEL detection kit (Beyotime, Shanghai, China) containing terminal deoxynucleotidyl
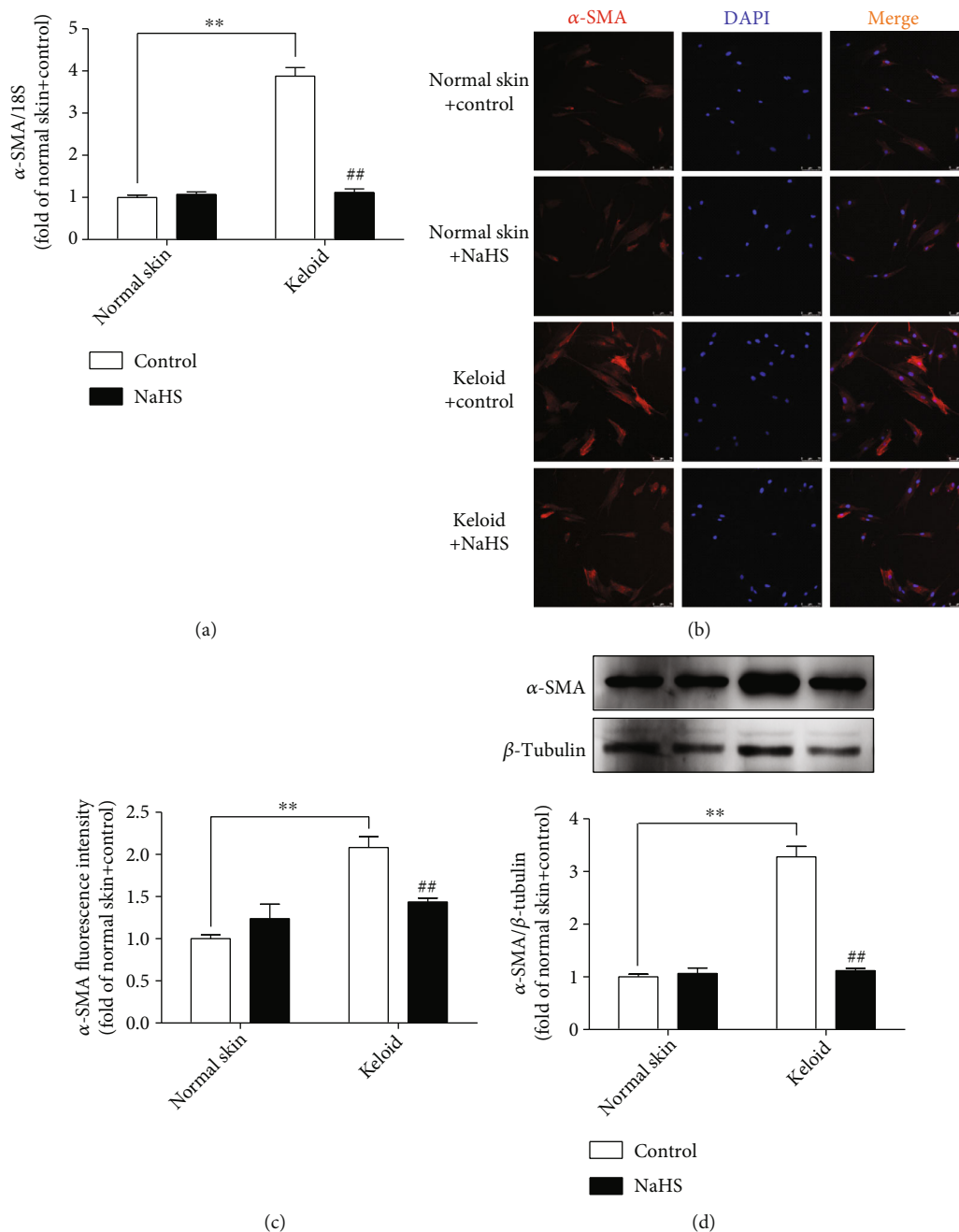
(a)

(b)

(c)

(d)

FIGURE 3: NaHS suppressed α-SMA expression in keloid fibroblasts. Skin fibroblasts were extracted from skin tissues of normal controls (normal skin) and scar tissue from patients with keloid (keloid), respectively. After pretreatment with NaHS ($50 \mu M$) or the same amount of culture medium (control) for 4 h, the fresh culture medium was replaced. (a) After 12 h, α-SMA mRNA expression was detected with real-time PCR. (b) α-SMA was immunofluorescence stained with Cy3- (red) conjugated IgG. The nuclei were stained with DAPI (blue). Bar = 75μm. (c) Quantitative statistics of α-SMA fluorescence intensity. (d) α-SMA protein expression was detected by Western blot. $^{**}P < 0.01$ vs. normal skin + control; $^{##}P < 0.01$ vs. keloid + control, $n = 6$.

transferase (TdT) and fluorescence agent at 37°C for 60 min in the dark. The fluorescence was photographed with a laser confocal microscope. The TUNEL-positive cells were calculated as the fold of the control group.

2.10. Real-Time PCR. Total RNA was extracted from skin fibroblasts with TRIzol. Then, RNA samples were sub-

jected to reverse transcription with the following procedure: 37°C for 15 min, 85°C for 5 sec, and 4°C forever. The cDNA was mixed with SYBR Green qPCR mixture (Takara, Otsu, Shiga, Japan) for further amplification (ABI 7500, ABI, Carlsbad, CA, USA). The primer sequences were listed as follows: α-SMA, sense 5$'$-GCGA TCTCACCGACTACCTG-3$'$ and antisense 5$'$-GCCGAC
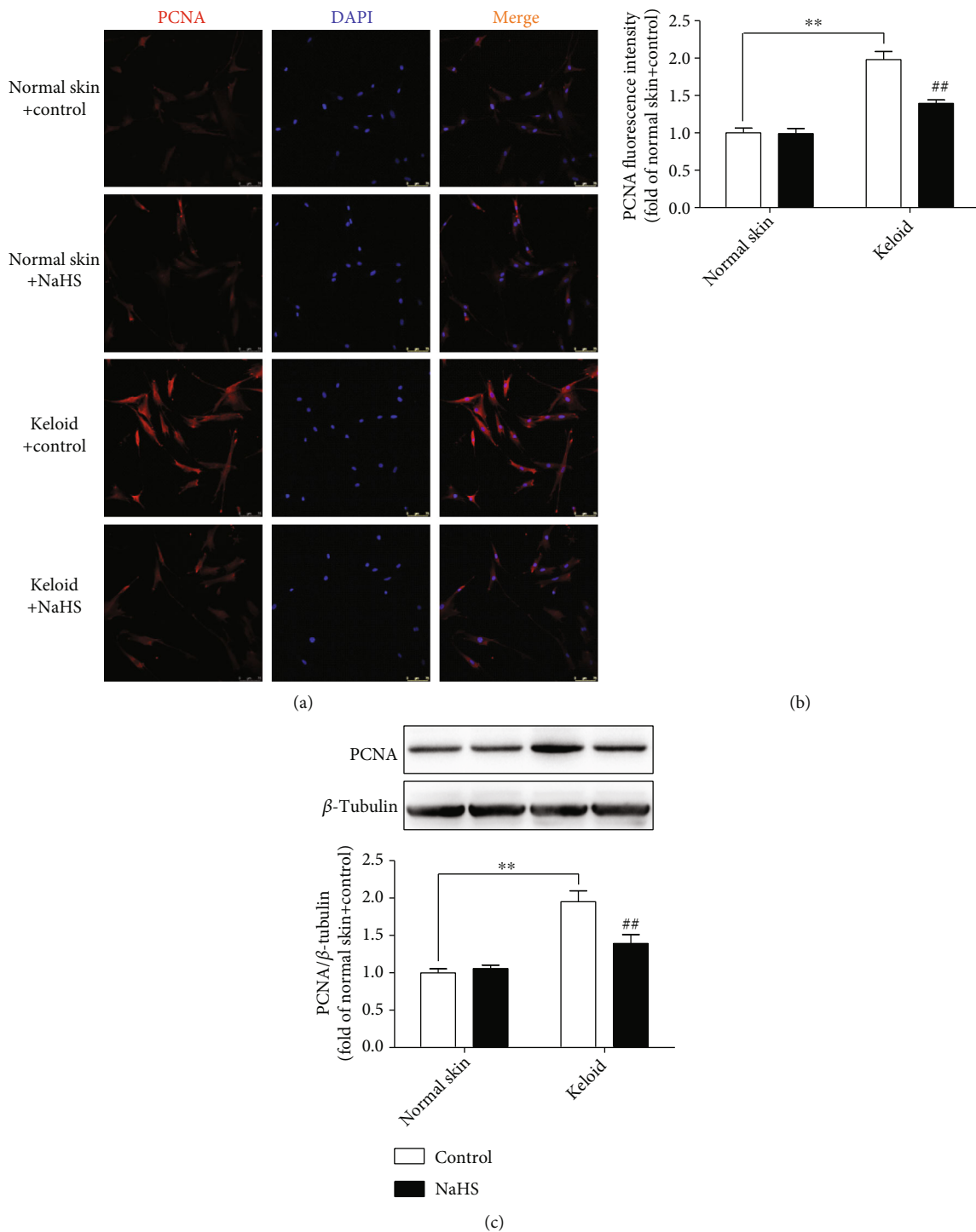
(a)

(b)

(c)

FIGURE 4: NaHS inhibited PCNA expression in keloid fibroblasts. Skin fibroblasts were extracted from skin tissues of normal controls (normal skin) and scar tissue from patients with keloid (keloid), respectively. After pretreatment with NaHS ($50\,\mu$M) or the same amount of culture medium (control) for 4 h, the fresh culture medium was replaced. (a) After 12 h, PCNA was immunofluorescence stained with Cy3- (red) conjugated IgG. The nuclei were stained with DAPI (blue). Bar $= 75\,\mu$m. (b) Quantitative statistics of PCNA fluorescence intensity. (c) Expression of PCNA protein was detected by Western Blot. $^{**}P < 0.01$ vs. normal skin + control; $^{\#\#}P < 0.01$ vs. keloid + control, $n = 6$.

TCCATACCGATGAA-3$'$; collagen I, sense 5$'$-AGACAT CCCACCAATCACCT-3$'$ and antisense 5$'$-CGTCATCGC ACAACACCTT-3$'$; collagen III, sense 5$'$-TGGCATCAA AGGACATCG-3$'$ and antisense 5$'$-CATAATACGGG GCAAAACC-3$'$; and 18S, sense 5$'$-AGTCCCTGCCCTTT GTACACA-3$'$ and antisense 5$'$-CGATCCGAGGGCCT CACTA-3$'$. The relative mRNA expression levels were calculated by the $\Delta\Delta$Ct method.
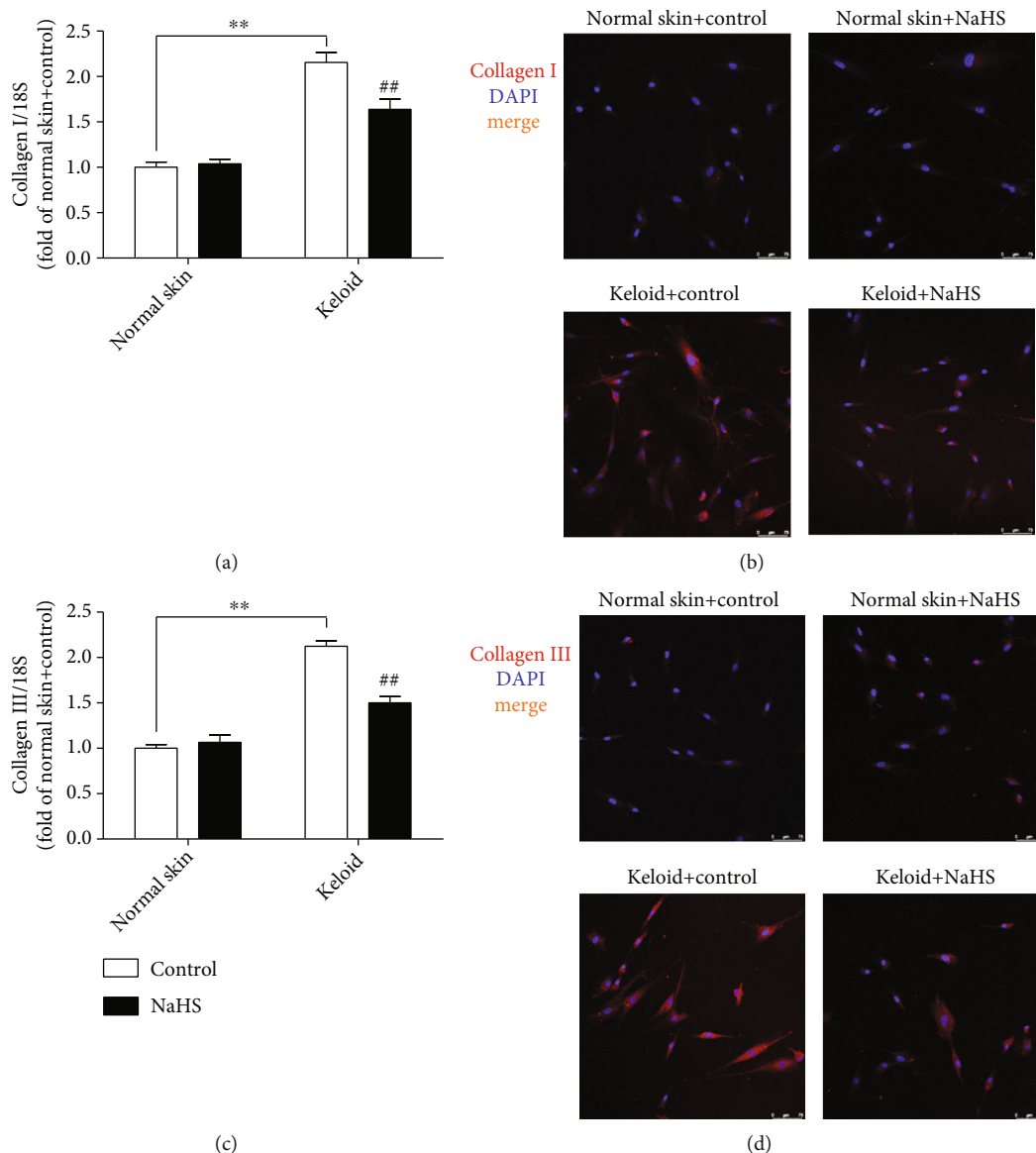
(a)

(b)

(c)

(d)

FIGURE 5: NaHS blocked collagen synthesis in keloid fibroblasts. Skin fibroblasts were extracted from skin tissues of normal controls (normal skin) and scar tissue from patients with keloid (keloid), respectively. After pretreatment with NaHS (50 μM) or the same amount of culture medium (control) for 4 h, the fresh culture medium was replaced. (a) After 12 h, collagen I mRNA expression was detected with real-time PCR. (b) Collagen I was immunofluorescence stained with Cy3- (red) conjugated IgG. The nuclei were stained with DAPI (blue). Bar = 75 μm. (c) Collagen III mRNA expression was detected with real-time PCR. (d) Collagen III was immunofluorescence stained with Cy3- (red) conjugated IgG. The nuclei were stained with DAPI (blue). Bar = 75 μm. $**P < 0.01$ vs. normal skin + control; $##P < 0.01$ vs. keloid + control, $n = 6$.

2.11. Western Blot.

The proteins from skin fibroblasts were separated by the sodium dodecyl sulphate- (SDS-) polyacrylamide gel electrophoresis (PAGE) and transferred to a polyvinylidene fluoride (PVDF, Millipore, Billerica, MA, USA) membrane. The membranes were blocked by 5% milk without fat for 2 h, then incubated with anti-α-SMA (1:2000; Bosterbio, Wuhan, China), anti-PCNA (1:2000; ABclonal, Wuhan, China), anti-receptor interacting protein kinase 1 (RIPK1), RIPK3, anti-mixed lineage kinase domain like protein (MLKL), p-MLKL (1:1000; Cell Signaling Technology, Danvers, MA, USA), anti-GAPDH (1:3000; Sigma-Aldrich, St. Louis, MO, USA),

anti-β-tubulin (1:3000; CMCTAG, Milwaukee, WI, USA), or anti-β-actin (1:5000; ABclonal, Wuhan, China) antibodies at 4°C overnight. Next, the secondary antibody (1:5000; Beyotime, Shanghai, china) was incubated for 2 h at room temperature. The protein bands were visualized on the membrane with enhanced chemiluminescence (ECL, Thermo Fisher Scientific Inc., Rockford, IL, USA) solution.

2.12. Statistical Analysis.

All data were expressed as the mean ± standard error of the mean (SEM) and analyzed by t test or one-way ANOVA followed by the Student-
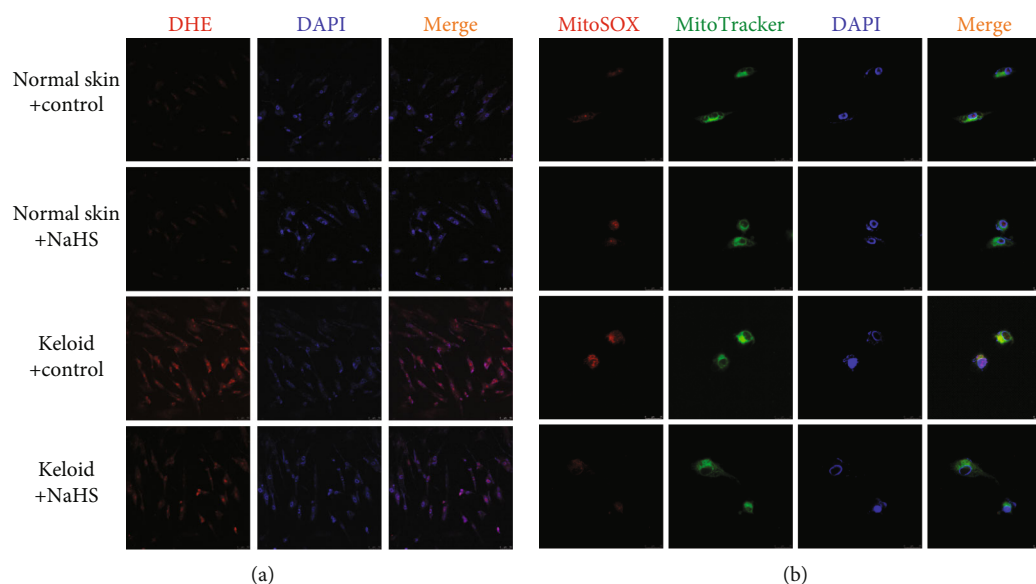
(a)   (b)

FIGURE 6: NaHS attenuated oxidative stress in keloid fibroblasts. Skin fibroblasts were extracted from skin tissues of normal controls (normal skin) and scar tissue from patients with keloid (keloid), respectively. After pretreatment with NaHS (50 μM) or the same amount of culture medium (control) for 4 h, the fresh culture medium was replaced. (a) After 12 h, intracellular superoxide anion was stained by DHE (red). The nuclei were stained with DAPI (blue). Bar = 50 μm. (b) Mitochondrial superoxide was stained with MitoSOX (red). The mitochondria were stained with MitoTracker (green). The nuclei were stained with DAPI (blue). Bar = 25 μm.
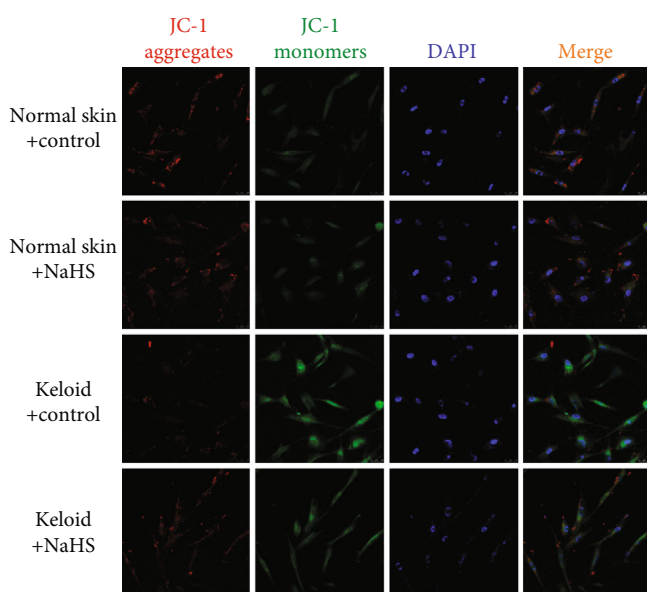

FIGURE 7: NaHS improved mitochondrial membrane potential in keloid fibroblasts. Skin fibroblasts were extracted from skin tissues of normal controls (normal skin) and scar tissue from patients with keloid (keloid), respectively. After pretreatment with NaHS (50 μM) or the same amount of culture medium (control) for 4 h, the fresh culture medium was replaced. After 12 h, mitochondrial membrane potential was detected by JC-1 staining. JC-1 aggregates (red) and JC-1 monomers (green) were observed. The nuclei were stained with DAPI (blue). Bar = 25 μm.

Newman-Keuls (SNK) test with the Stata 13.0 software. The value of P less than 0.05 was considered significant difference.

3. Results

3.1. H_2S Production Is Impaired in Patients with Keloid. H_2S levels were measured in plasma and skin tissues of patients. There were lower plasma H_2S content and skin H_2S production in patients with keloid than that in normal control ($P < 0.01$) (Figure 1), suggesting that H_2S production was impaired in patients with keloid.

3.2. NaHS Inhibits Keloid Fibroblast Migration after Scratch. However, whether impaired H_2S production was critical in the pathological process of keloid was unknown. Next, we investigated the influence of restoring H_2S level on keloid fibroblast proliferation. The scratch migration assay showed that the migration rate of keloid fibroblasts after scratch was faster than that of normal skin fibroblasts ($P < 0.01$), which was significantly reduced by NaHS pretreatment ($P < 0.01$) (Figure 2). It suggested that exogenous H_2S supplementation inhibited keloid fibroblast migration after scratch.

3.3. NaHS Suppresses α-SMA Expression in Keloid Fibroblasts. α-SMA is one of the sensitive markers to indicate cells proliferation [26]. Therefore, the expression of α-SMA was detected in cells with real-time PCR, immunofluorescence, and Western blot. All these results consistently showed that there was more α-SMA expression in keloid fibroblasts than that in normal skin fibroblasts ($P < 0.01$), which was significantly suppressed by NaHS pretreatment ($P < 0.01$) (Figure 3). It demonstrated that exogenous H_2S supplementation inhibited keloid fibroblast proliferation.
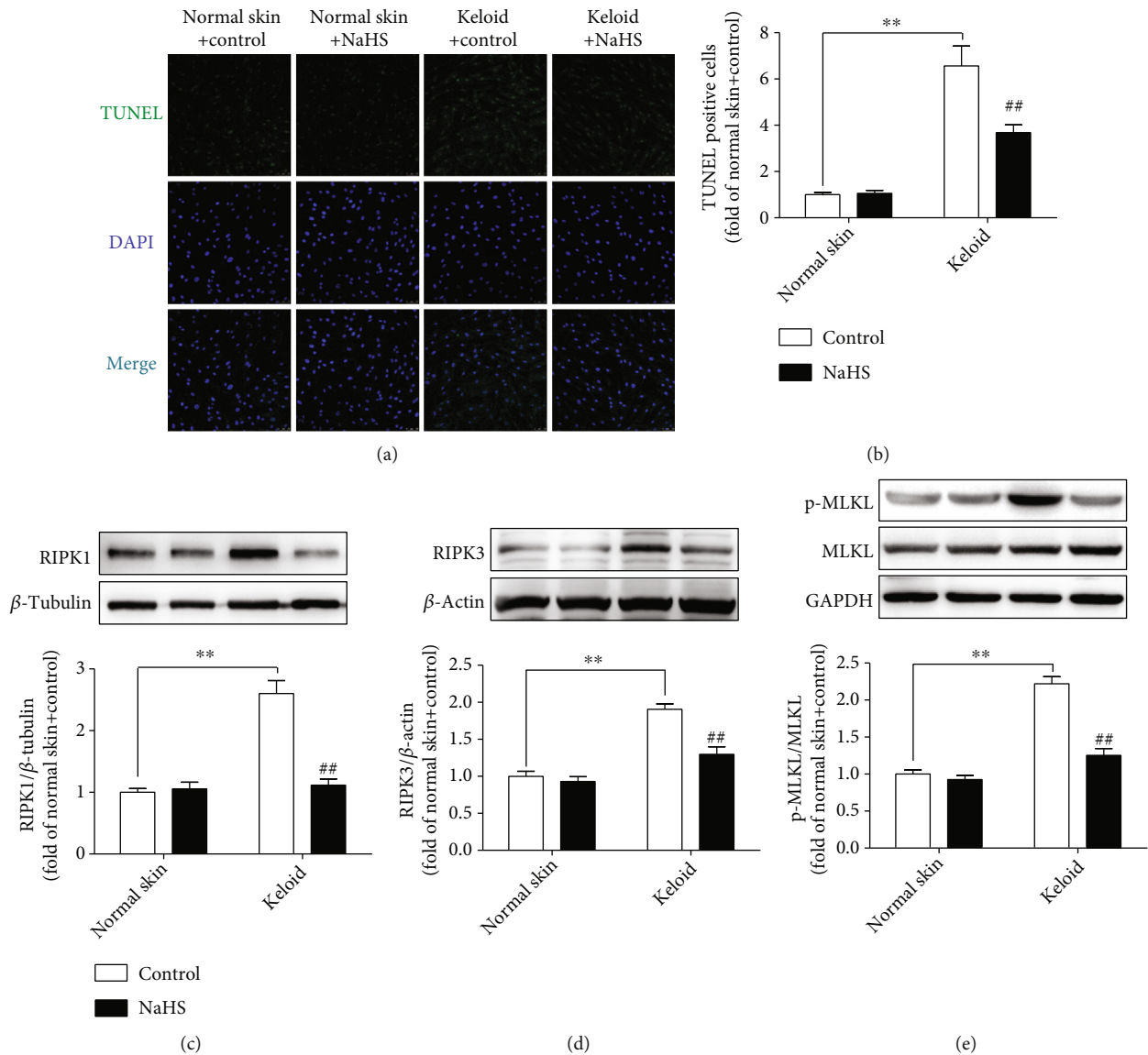
(a)

(b)

(c)

(d)

(e)

FIGURE 8: NaHS alleviated necroptosis in keloid fibroblasts. Skin fibroblasts were extracted from skin tissues of normal controls (normal skin) and scar tissue from patients with keloid (keloid), respectively. After pretreatment with NaHS (50 μM) or the same amount of culture medium (control) for 4 h, the fresh culture medium was replaced. (a) After 12 h, necroptotic cells were marked with TUNEL staining (green). The nuclei were stained with DAPI (blue). Bar = 50 μm. (b) Quantitative statistics of TUNEL-positive cells. (c–e) Expression of RIPK1, RIPK3, and MLKL was detected by Western blot. $^{**}P < 0.01$ vs. normal skin + control; $^{##}P < 0.01$ vs. keloid + control, $n = 6$.

3.4. NaHS Inhibits PCNA Expression in Keloid Fibroblasts. PCNA, another sensitive indicator of skin fibroblast proliferation, plays an important role in DNA replication [27]. Therefore, PCNA was also detected to verify the influence of H$_2$S on keloid fibroblast proliferation. Real-time PCR, immunofluorescence, and Western blot demonstrated that PCNA expression was higher in keloid fibroblasts than that in normal skin fibroblasts ($P < 0.01$), which was significantly suppressed by NaHS pretreatment ($P < 0.01$) (Figure 4), further indicating that exogenous H$_2$S supplementation inhibited keloid fibroblast proliferation.

3.5. NaHS Blocks Collagen Synthesis in Keloid Fibroblasts. Then, the content of collagen I and collagen III was measured to evaluate the influence of H$_2$S on collagen synthesis.

Both real-time PCR and immunofluorescence verified that compared with normal skin fibroblasts, the expression of collagen I and collagen III in keloid fibroblasts was significantly higher than that in normal skin fibroblasts ($P < 0.01$), which was reduced by NaHS pretreatment ($P < 0.01$) (Figure 5). It suggested that exogenous H$_2$S supplementation blocked collagen synthesis in keloid fibroblasts.

3.6. NaHS Attenuates Oxidative Stress in Keloid Fibroblasts. DHE staining and MitoSOX staining were applied to detect the level of intracellular superoxide anion and mitochondrial superoxide, respectively. Compared with normal skin fibroblasts, red fluorescence by DHE and MitoSOX staining in keloid fibroblasts was stronger, which was weakened by NaHS pretreatment (Figure 6), demonstrating that
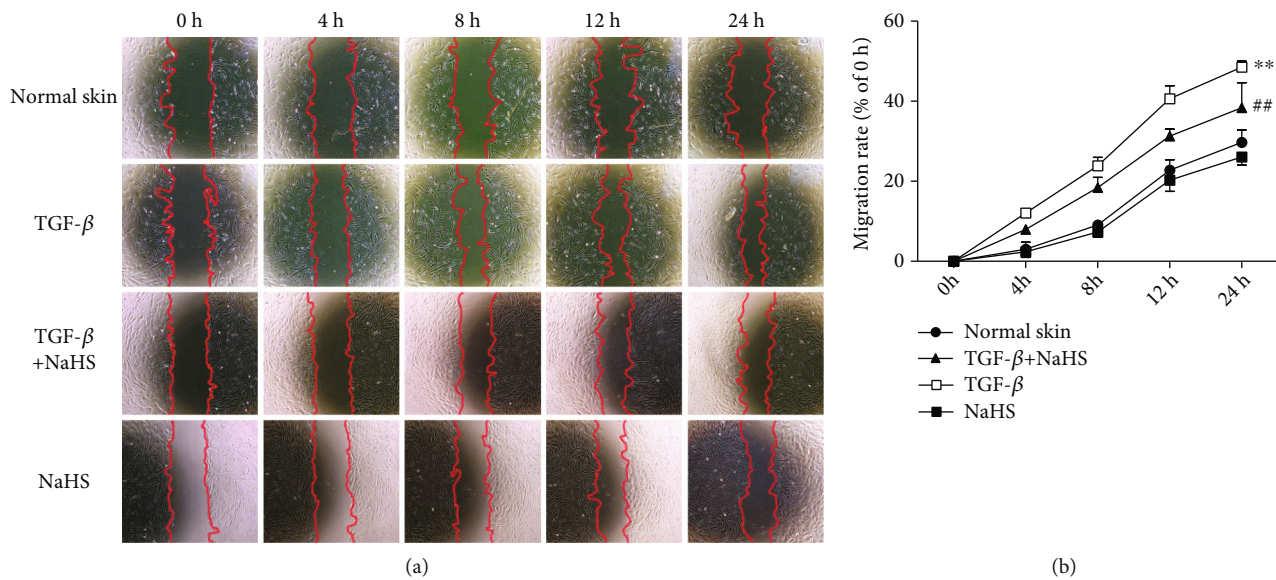
(a)

(b)

FIGURE 9: NaHS inhibited TGF-β_1-stimulated skin fibroblast migration after scratch. Skin fibroblasts were extracted from skin tissues of normal controls (normal skin). After pretreatment with NaHS (50 μM) for 4 h, skin fibroblasts were stimulated with TGF-β_1 (10 ng/mL) for 12 h. The cells were scratched with 10 μL pipette tip. (a) Photos were taken after scratch for 0 h, 4 h, 8 h, 12 h, and 24 h. (b) The percentage of cell migration area to initial scratch area at different time. $^{**}P < 0.01$ vs. normal skin; $^{\#\#}P < 0.01$ vs. TGF-β_1, $n = 6$.

intracellular superoxide anion and mitochondrial superoxide were both inhibited by NaHS. It suggested that exogenous H$_2$S supplementation attenuated oxidative stress in keloid fibroblasts.

3.7. NaHS Improves Mitochondrial Membrane Potential in Keloid Fibroblasts.

Decreased mitochondrial membrane potential ($\Delta\psi$m) might contribute to mitochondrial injury and ROS accumulation [28]. Red fluorescence by JC-1 staining indicated normal mitochondria with higher $\Delta\psi$m, while green indicated impaired mitochondria with lower $\Delta\psi$m. Our experiment demonstrated that compared with normal skin fibroblasts, green fluorescence was increased, but red fluorescence was decreased in keloid fibroblasts, while NaHS pretreatment significantly enhanced red and weakened green fluorescence (Figure 7), suggesting that exogenous H$_2$S supplementation improved mitochondrial membrane potential to alleviate mitochondrial damage in keloid fibroblasts.

3.8. NaHS Alleviates Necroptosis in Keloid Fibroblasts.

Due to the intercellular genomic DNA breakage and 3′ OH exposing at the early stage, apoptotic cells were able to be marked by TUNEL staining, which is also one characteristic of necroptosis [29]. Necroptosis is strictly regulated by multiple molecules. RIPK1 and RIPK3, two key signal molecules to mediate necroptosis, are commonly considered specific indicators of necroptosis. In addition, MLKL is a core substrate of RIPK3 downstream to mediate necroptosis. Therefore, TUNEL staining and the above proteins measurement were applied to evaluate cell necroptosis. Compared with normal skin fibroblasts, there were more TUNEL staining-positive cells, higher RIPK1 and RIPK3 expressions as well as MLKL phosphorylation in keloid fibroblasts ($P < 0.01$),

which were all reversed by NaHS pretreatment ($P < 0.01$) (Figure 8). These data indicated that exogenous H$_2$S supplementation alleviated necroptosis in keloid fibroblasts.

3.9. NaHS Inhibits TGF-β_1-Stimulated Skin Fibroblast Migration after Scratch.

The above results demonstrated that exogenous H$_2$S supplementation inhibited keloid fibroblast proliferation. However, whether the above effects could be extended to other dermatofibrotic diseases is unknown. Therefore, normal skin fibroblasts were extracted and stimulated with TGF-β_1. Skin fibroblast migration with TGF-β_1 stimulation after scratch was faster than normal skin fibroblasts ($P < 0.01$), which was reversed by NaHS pretreatment ($P < 0.01$) (Figure 9). It suggested that exogenous H$_2$S supplementation inhibited TGF-β_1 stimulated skin fibroblast migration after scratch.

3.10. NaHS Suppresses α-SMA Expression in TGF-β_1-Stimulated Skin Fibroblasts.

Compared with normal skin fibroblasts, there were more α-SMA expression after TGF-β_1 stimulation ($P < 0.01$), which was decreased by NaHS pretreatment ($P < 0.01$) (Figure 10), suggesting that exogenous H$_2$S supplementation suppressed TGF-β_1-stimulated skin fibroblast proliferation.

3.11. NaHS Inhibits PCNA Expression in TGF-β_1-Stimulated Skin Fibroblasts.

Compared with normal skin fibroblasts, there were higher PCNA expression after TGF-β_1 stimulation ($P < 0.01$), which was inhibited by NaHS pretreatment ($P < 0.01$) (Figure 11), further indicating that exogenous H$_2$S supplementation suppressed TGF-β_1-stimulated skin fibroblast proliferation.

3.12. NaHS Blocks Collagen Synthesis in TGF-β_1-Stimulated Skin Fibroblasts.

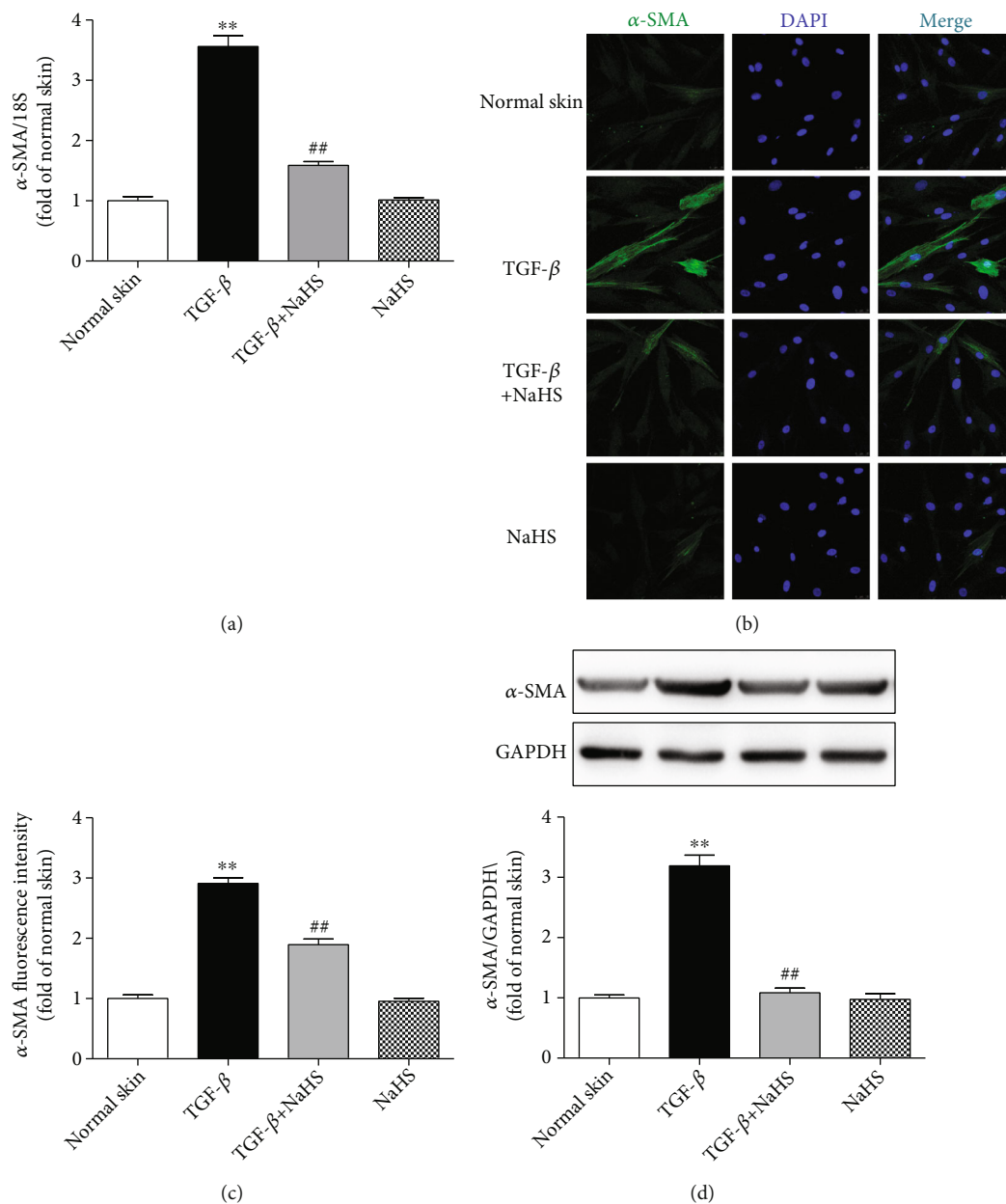Compared with normal skin fibroblasts,

(a)

(b)

(c)

(d)

FIGURE 10: NaHS suppressed α-SMA expression in TGF-β_1-stimulated fibroblasts. Skin fibroblasts were extracted from skin tissues of normal controls (normal skin). After pretreatment with NaHS (50 μM) for 4 h, skin fibroblasts were stimulated with TGF-β_1 (10 ng/mL) for 12 h. (a) α-SMA mRNA expression was detected with real-time PCR. (b) α-SMA was immunofluorescence stained with Alexa Fluor 488- (green) conjugated IgG. The nuclei were stained with DAPI (blue). Bar = 25 μm. (c) Quantitative statistics of α-SMA fluorescence intensity. (d) α-SMA protein expression was detected by Western blot. $^{**}P < 0.01$ vs. normal skin; $^{##}P < 0.01$ vs. TGF-β_1, $n = 6$.

there were more collagen I and collagen III expressions after TGF-β_1 stimulation ($P < 0.01$), which was suppressed by NaHS pretreatment ($P < 0.01$) (Figure 12), indicating that exogenous H$_2$S supplementation blocked TGF-β_1-stimulated skin fibroblast collagen synthesis.

3.13. NaHS Attenuates Oxidative Stress in TGF-β_1-Stimulated Skin Fibroblasts. Compared with normal skin fibroblasts, TGF-β_1 stimulation enhanced red fluorescence in skin fibroblasts, which was weakened by NaHS pretreatment (Figure 13), and demonstrated that intracellular super-

oxide anion and mitochondrial superoxide were inhibited by NaHS. It suggested that exogenous H$_2$S supplementation attenuated oxidative stress in TGF-β_1-stimulated skin fibroblasts.

3.14. NaHS Alleviates Necroptosis in TGF-β_1-Stimulated Skin Fibroblasts. Compared with normal skin fibroblasts, TGF-β_1 stimulation increased the positive rate of TUNEL staining and upregulated RIPK1 and RIPK3 expressions as well as MLKL phosphorylation ($P < 0.01$), which were all reversed by NaHS pretreatment ($P < 0.01$) (Figure 14).

(a)

(b)

(c)
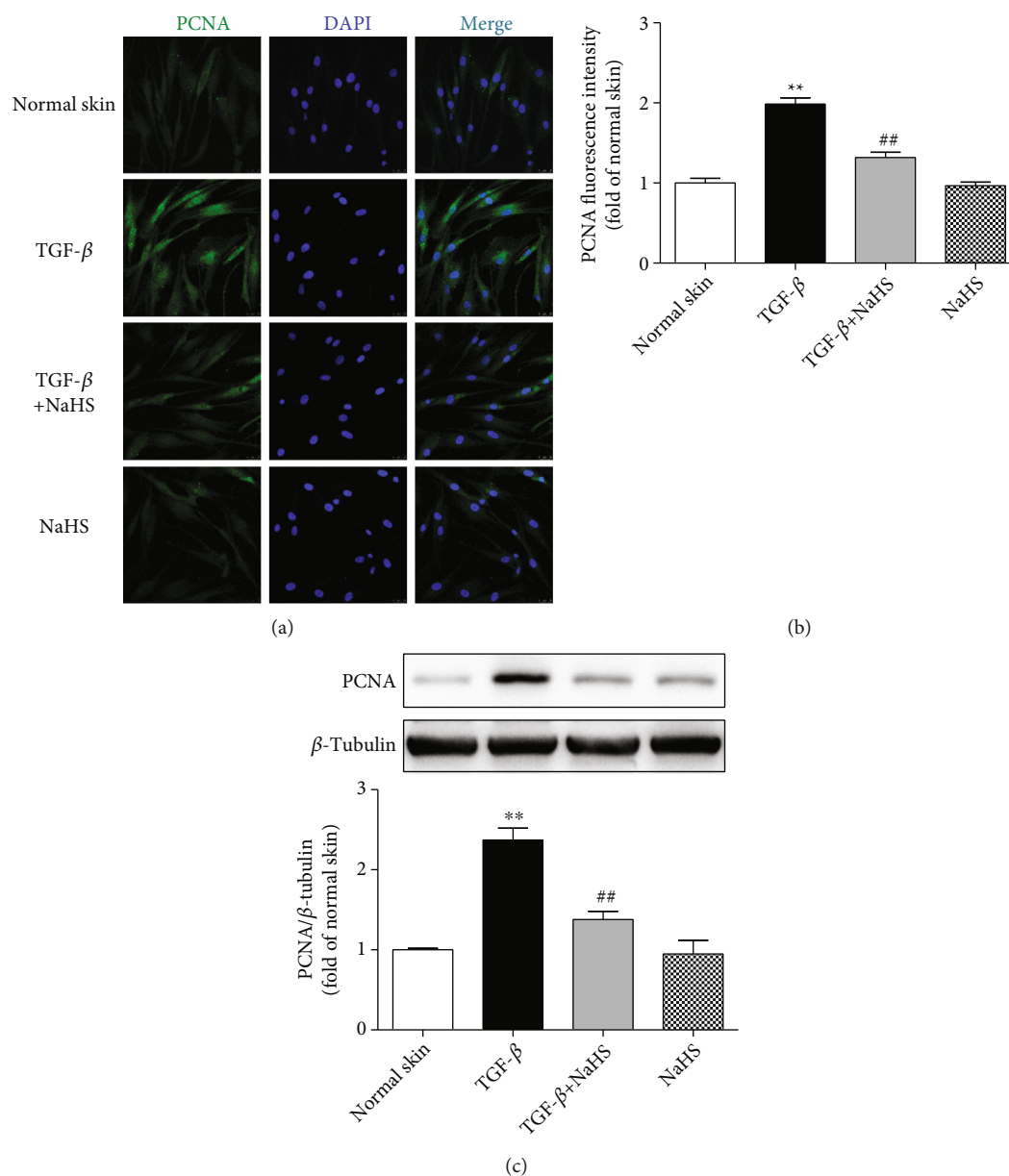
FIGURE 11: NaHS inhibited PCNA expression in TGF-β_1-stimulated fibroblasts. Skin fibroblasts were extracted from skin tissues of normal controls (normal skin). After pretreatment with NaHS (50 μM) for 4 h, skin fibroblasts were stimulated with TGF-β_1 (10 ng/mL) for 12 h. (a) PCNA was immunofluorescence stained with Alexa Fluor 488- (green) conjugated IgG. The nuclei were stained with DAPI (blue). Bar = 25 μm. (b) Quantitative statistics of PCNA fluorescence intensity. (c) PCNA protein expression was detected by Western blot. $^{**}P < 0.01$ vs. normal skin; $^{\#\#}P < 0.01$ vs. TGF-β_1, $n = 6$.

These results suggested that exogenous H$_2$S supplementation alleviated necroptosis in TGF-β_1-stimulated skin fibroblasts.

4. Discussion

As an endogenous gasotransmitter, H$_2$S plays an important role in a variety of pathophysiological processes. H$_2$S dysfunction is reported to be involved in the pathogenesis of hypertension, diabetes, atherosclerosis, and tumor [30–32]. Previous studies showed that excessive H$_2$S production induced thyroid malignancy, deteriorated pancreatitis, and

lung injury [33, 34], while impaired H$_2$S production promoted obesity and aggravated insulin resistance [35]. In addition, H$_2$S content was significantly decreased in patients with psoriasis, which was negatively correlated with the severity of clinical symptoms [36, 37]. H$_2$S also facilitated melanoma cell apoptosis and inhibited tumor growth by upregulating Fas-associated protein with a novel death domain (FADD) [38]. Exogenous H$_2$S suppressed melanoma cells migration and invasion to delay melanoma progression and metastasis formation [39]. Interestingly, a novel drug carrier nanofibrous membrane, blending the recombinant spider silk protein and NaHS by electrospun,
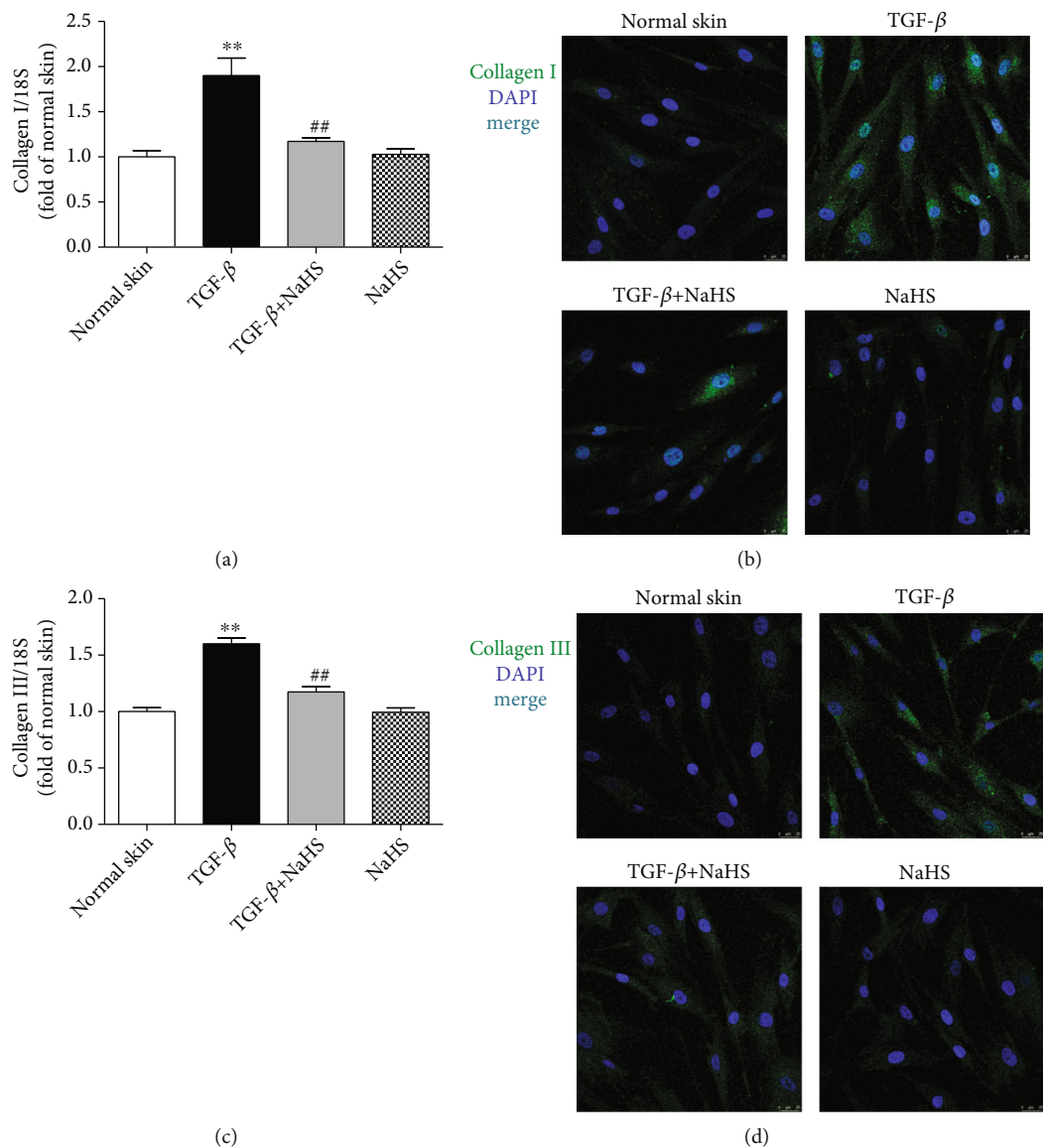
(a)

(b)

(c)

(d)

Figure 12: NaHS prevented collagen synthesis in TGF-β_1-stimulated fibroblasts. Skin fibroblasts were extracted from skin tissues of normal controls (normal skin). After pretreatment with NaHS (50 μM) for 4 h, skin fibroblasts were stimulated with TGF-β_1 (10 ng/mL) for 12 h. (a) Collagen I mRNA expression was detected with real-time PCR. (b) Collagen I was immunofluorescence stained with Alexa Fluor 488- (green) conjugated IgG. The nuclei were stained with DAPI (blue). Bar = 25 μm. (c) Collagen III mRNA expression was detected with real-time PCR. (d) Collagen III was immunofluorescence stained with Alexa Fluor 488- (green) conjugated IgG. The nuclei were stained with DAPI (blue). Bar = 25 μm. $^{**}P < 0.01$ vs. normal skin; $^{\#\#}P < 0.01$ vs. TGF-β_1, $n = 6$.

promoted skin wound healing [40]. These studies suggest that H$_2$S has a potential effect on skin diseases.

Keloid is a skin benign fibroproliferative disease, and the definite pathogenesis of keloid is not clear. We found that the H$_2$S level in the plasma and skin of patients with keloid was notably decreased, suggesting that H$_2$S production impairment might be involved in human skin fibroblast proliferation. Previous studies have verified that H$_2$S improved multiple fibrotic diseases. Specifically, exogenous H$_2$S prevented myocardial fibrosis during myocardial infarction, hypertension, and diabetes [41]. H$_2$S also attenuated vascular fibrosis by regulating endothelial mesenchymal transition (EndMT) [42]. H$_2$S alleviated hypoxia-induced chronic

renal fibrosis *via* restoring ten-eleven translocations (TET), reversing DNA methylation, and enhancing Klotho gene expression [43]. Our present study found that NaHS pretreatment slowed down keloid fibroblast migration, decreased the expression of α-SMA, PCNA, collagen I, and collagen III. It suggested that exogenous H$_2$S supplementation inhibited keloid fibroblast proliferation. Then we further explored the possible effect of H$_2$S on some other fibrotic diseases. It is widely known that the excess activation of TGF-β_1 signaling pathway contributed to the occurrence and development of dermatofibrotic diseases including keloid [44]. Therefore, TGF-β_1 stimulation is a common experimental strategy to induce skin fibroblast proliferation
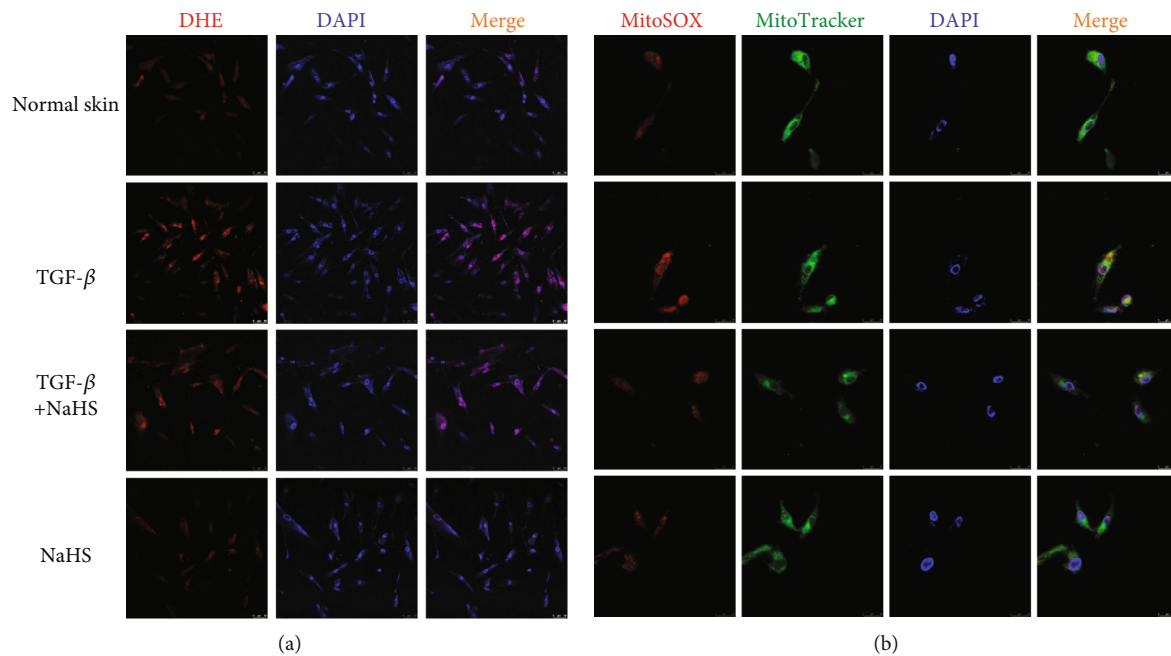
FIGURE 13: NaHS attenuated oxidative stress in TGF-β_1-stimulated skin fibroblasts. Skin fibroblasts were extracted from skin tissues of normal controls (normal skin). After pretreatment with NaHS (50 μM) for 4 h, skin fibroblasts were stimulated with TGF-β_1 (10 ng/mL) for 12 h. (a) The intracellular superoxide anion was stained by DHE (red). The nuclei were stained with DAPI (blue). Bar = 50 μm. (b) Mitochondrial superoxide was stained with MitoSOX (red). The mitochondria were stained with MitoTracker (green). The nuclei were stained with DAPI (blue). Bar = 25 μm.

and imitate dermatofibrotic diseases. Our results showed that TGF-β_1 stimulation accelerated skin fibroblast migration and upregulated the expression of α-SMA, PCNA, collagen I, and collagen III, suggesting that TGF-β_1 successfully induced critical characteristics of skin fibrosis *in vitro*. Similar to the preventive effects against keloid fibroblasts, NaHS pretreatment also inhibited cell migration and suppressed the expression of α-SMA, PCNA, collagen I, and collagen III in TGF-β_1-stimulated skin fibroblasts. Taken together, the above evidence indicates that H$_2$S possibly has a powerful therapeutic effect on skin fibrosis, which is conducive to developing novel ideas for the prevention and treatment of dermatofibrotic diseases.

Previous studies verified that H$_2$S attenuated oxidative stress, regulated glucose and fat metabolism, and improved mitochondrial function to alleviate liver cirrhosis [45]. H$_2$S inhibited inflammation and oxidative stress, reduced the expression of Toll like receptor 4 (TLR4), NOD like receptor family pyrin domain containing 3 (NLRP3), and caspase-1, improved the renal function and renal histopathological changes, and alleviated kidney injury in sepsis-associated acute kidney injury (SA-AKI) [46]. H$_2$S also inhibited oxidative stress to correct the dysfunction in neurodegenerative diseases [47]. H$_2$S attenuated paraquat-induced acute liver injury *via* enhancing antioxidant capacity, regulating mitochondrial function, and inhibiting NLRP3 inflammasome activation [48]. All these studies indicated that the antioxidant effect of H$_2$S might be one of the common mechanisms to improve fibrosis in various organs and tissues. DHE, MitoSOX, and JC-1 staining in our experiment confirmed that NaHS pretreatment decreased intracellular superoxide

anion and mitochondrial superoxide but increased mitochondrial membrane potential in keloid fibroblasts and TGF-β_1-stimulated normal skin fibroblasts, suggesting that exogenous H$_2$S supplementation attenuated oxidative stress. These results indicated that the antiproliferation effect of H$_2$S on skin fibroblasts might be ascribed to oxidative stress inhibition.

Intracellular ROS accumulation can induce cell necroptosis, which is a new type of programmed cell death with the characteristics of both apoptosis and necrosis. Necroptosis plays an important role in maintaining cell homeostasis, regulating tumor immunity and inflammatory response, and mediating ischemic injury and several other pathophysiological processes [49, 50]. As two important mediators of necroptosis, RIPK1 combines with RIPK3 to form necrosomes and phosphorylate MLKL, which then transfers to cell membrane and ruptures it, and exaggerates cell necroptosis finally [51]. Due to the enhanced oxidative stress, necroptosis was consequently increased in mice with chronic hepatitis [52]. Some researchers found that ROS accumulation in melanocytes' mitochondria promoted necrosome formation and aggravated necroptosis in the pathogenesis of vitiligo [53]. Our present experiment showed that NaHS pretreatment downregulated the expression of RIPK1 and RIPK3, inhibited MLKL phosphorylation, and decreased the TUNEL staining-positive rate in keloid fibroblasts and TGF-β_1-stimulated normal skin fibroblasts, suggesting that exogenous H$_2$S supplementation alleviated necroptosis in both keloid fibroblasts and TGF-β_1-stimulated normal skin fibroblasts. However, besides expression of RIPK1, RIPK3, and MLKL, some other proteins including cleaved caspase
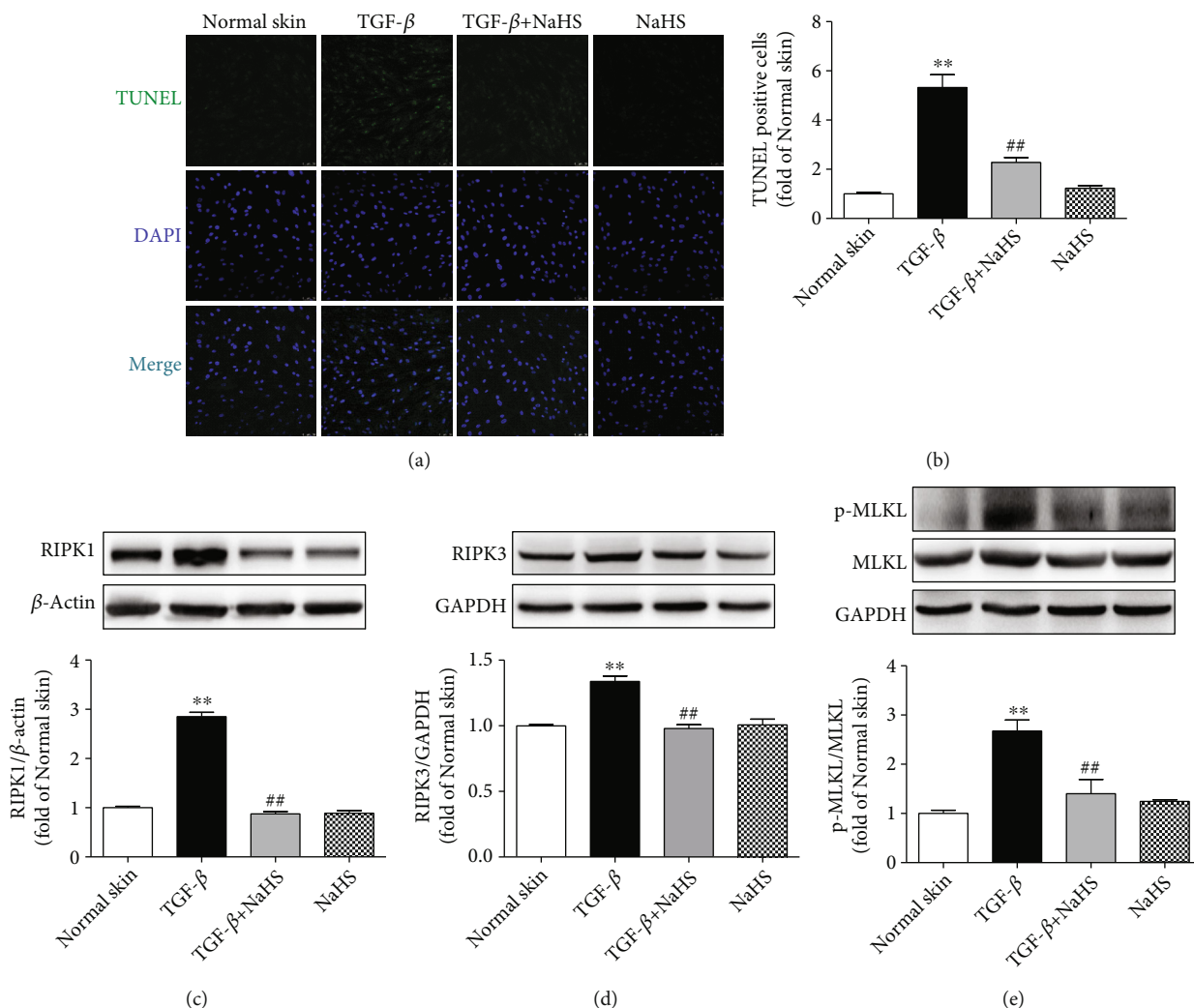
FIGURE 14: NaHS alleviated necroptosis in TGF-β_1-stimulated skin fibroblasts. Skin fibroblasts were extracted from skin tissues of normal controls (normal skin). After pretreatment with NaHS (50 μM) for 4 h, skin fibroblasts were stimulated with TGF-β_1 (10 ng/mL) for 12 h. (a) Necroptotic cells were marked with TUNEL staining (green). The nuclei were stained with DAPI (blue). Bar = 50 μm. (b) Quantitative statistics of TUNEL-positive cells. (c–e) Expression of RIPK1, RIPK3, and MLKL was detected by Western blot. $^{**}P < 0.01$ vs. normal skin; $^{##}P < 0.01$ vs. TGF-β_1, $n = 6$.

3, necrosomes, and inflammasomes had not been detected in our present study. Actually, more necroptosis proteins will be a great benefit to validate the effect of H$_2$S on necroptosis in skin fibroblasts. This is one limitation of our present study. Considering the powerful antioxidant effects, the suppressive ability of necroptosis by H$_2$S may be attributed to the inhibition of oxidative stress. Interestingly, inhibition of skin fibroblasts necroptosis by H$_2$S seems to contradict with the preventive effects on proliferation. Actually, a large amount of cellular contents will be released after necroptosis, such as inflammatory factors, cell metabolites, and other substances, which all further promote cell proliferation. Recently, some researchers found that H$_2$S attenuated necroptosis depending on sirtuin3 enhancement to suppress excessive proliferation in hypoxia-induced cardiac fibroblasts [25]. That is to say that the mutual regulation between cell death and proliferation is very complex. Therefore, the inhibitory mechanism of H$_2$S on skin fibroblast proliferation

may involve some other reactions, such as extracellular matrix degradation, inflammation aggravation, and cytokine release, which need future research.

In conclusion, H$_2$S production was impaired in the plasma and skin of patients with keloid. Exogenous H$_2$S supplementation suppressed proliferation in keloid fibroblasts and TGF-β_1-stimulated normal skin fibroblasts. The suppressive mechanisms may be related to oxidative stress alleviation and necroptosis inhibition. Our present study is of benefit to provide a novel strategy for the prevention and treatment of keloid and some other dermatofibrotic diseases.

Data Availability

The data used to support the finding of this study are available from the corresponding authors upon request.

Conflicts of Interest

The authors declare that there is no conflict of interest regarding the publication of this paper.

Authors' Contributions

Ling Li and Ziying He contributed equally to this study.

Acknowledgments

References

[1] A. Hawash, G. Ingrasci, K. Nouri, and G. Yosipovitch, "Pruritus in keloid scars: mechanisms and treatments," *Acta Dermato Venereologica*, vol. 101, no. 10, article adv00582, 2021.

[2] S. Ud-Din and A. Bayat, "Keloid scarring or disease: unresolved quasi-neoplastic tendencies in the human skin," *Wound Repair and Regeneration*, vol. 28, no. 3, pp. 422–426, 2020.

[3] M. L. Elsaie, "Update on management of keloid and hypertrophic scars: a systemic review," *Journal of Cosmetic Dermatology*, vol. 20, no. 9, pp. 2729–2738, 2021.

[4] S. F. Ekstein, S. P. Wyles, S. L. Moran, and A. Meves, "Keloids: a review of therapeutic management," *International Journal of Dermatology*, vol. 60, no. 6, pp. 661–671, 2021.

[5] T. Zhang, X. F. Wang, Z. C. Wang et al., "Current potential therapeutic strategies targeting the TGF-β/Smad signaling pathway to attenuate keloid and hypertrophic scar formation," *Biomedicine & Pharmacotherapy*, vol. 129, article 110287, 2020.

[6] H. H. Hu, D. Q. Chen, Y. N. Wang et al., "New insights into TGF-β/Smad signaling in tissue fibrosis," *Chemico-Biological Interactions*, vol. 292, pp. 76–83, 2018.

[7] J. M. Carthy, "TGFβ signaling and the control of myofibroblast differentiation: Implications for chronic inflammatory disorders," *Journal of Cellular Physiology*, vol. 233, no. 1, pp. 98–106, 2018.

[8] E. Zaorska, L. Tomasova, D. Koszelewski, R. Ostaszewski, and M. Ufnal, "Hydrogen sulfide in pharmacotherapy, beyond the hydrogen sulfide-donors," *Biomolecules*, vol. 10, no. 2, article 323, 2020.

[9] M. Xu, L. Zhang, S. Song et al., "Hydrogen sulfide: recent progress and perspectives for the treatment of dermatological diseases," *Journal of Advanced Research*, vol. 27, pp. 11–17, 2021.

[10] Q. Xiao, L. Xiong, J. Tang, L. Li, and L. Li, "Hydrogen sulfide in skin diseases: a novel mediator and therapeutic target," *Oxidative Medicine and Cellular Longevity*, vol. 2021, Article ID 6652086, 11 pages, 2021.

[11] R. V. Pinto, S. Carvalho, F. Antunes, J. Pires, and M. L. Pinto, "Emerging nitric oxide and hydrogen sulfide releasing carriers for skin wound healing therapy," *ChemMedChem*, vol. 17, no. 1, article e202100429, 2022.

[12] M. Xu, Y. Hua, Y. Qi, G. Meng, and S. Yang, "Exogenous hydrogen sulphide supplement accelerates skin wound healing via oxidative stress inhibition and vascular endothelial growth factor enhancement," *Experimental Dermatology*, vol. 28, no. 7, pp. 776–785, 2019.

[13] G. Wang, W. Li, Q. Chen, Y. Jiang, X. Lu, and X. Zhao, "Hydrogen sulfide accelerates wound healing in diabetic rats," *International Journal of Experimental Pathology*, vol. 8, no. 5, pp. 5097–5104, 2015.

[14] H. Zhao, S. Lu, J. Chai et al., "Hydrogen sulfide improves diabetic wound healing in ob/ob mice via attenuating inflammation," *Journal of Diabetes and its Complications*, vol. 31, no. 9, pp. 1363–1369, 2017.

[15] L. Rodrigues, E. Ekundi-Valentim, J. Florenzano et al., "Protective effects of exogenous and endogenous hydrogen sulfide in mast cell- mediated pruritus and cutaneous acute inflammation in mice," *Pharmacological Research*, vol. 115, pp. 255–266, 2017.

[16] G. Ercolano, P. De Cicco, F. Frecentese et al., "Anti-metastatic properties of naproxen-HBTA in a murine model of cutaneous melanoma," *Frontiers in Pharmacology*, vol. 10, article 66, 2019.

[17] P. De Cicco, E. Panza, G. Ercolano et al., "ATB-346, a novel hydrogen sulfide-releasing anti-inflammatory drug, induces apoptosis of human melanoma cells and inhibits melanoma development in vivo," *Pharmacological Research*, vol. 114, pp. 67–73, 2016.

[18] Y. Huang, Z. Zhang, Y. Huang et al., "Induction of inactive TGF-β1 monomer formation by hydrogen sulfide contributes to its suppressive effects on Ang II- and TGF-β1-induced EMT in renal tubular epithelial cells," *Biochemical & Biophysical Research Communications*, vol. 501, no. 2, pp. 534–540, 2018.

[19] F. Z. Wang, H. Zhou, H. Y. Wang et al., "Hydrogen sulfide prevents arterial medial calcification in rats with diabetic nephropathy," *BMC Cardiovascular Disorders*, vol. 21, no. 1, pp. 1–11, 2021.

[20] H. Tran, Y. Yu, L. Chang et al., "A novel liposomal s-propargyl-cysteine: a sustained release of hydrogen sulfide reducing myocardial fibrosis via TGF-β1/Smad pathway," *International Journal of Nanomedicine*, vol. 14, pp. 10061–10077, 2019.

[21] L. Wang, J. Meng, C. Wang et al., "Hydrogen sulfide alleviates cigarette smoke-induced COPD through inhibition of the TGF-β1/Smad pathway," *Experimental Biology and Medicine*, vol. 245, no. 3, pp. 190–200, 2020.

[22] R. Guan, J. Wang, Z. Cai et al., "Hydrogen sulfide attenuates cigarette smoke-induced airway remodeling by upregulating SIRT1 signaling pathway," *Redox Biology*, vol. 28, article 101356, 2020.

[23] S. S. Chirindoth and I. Cancarevic, "Role of hydrogen sulfide in the treatment of fibrosis," *Cureus*, vol. 13, no. 9, article e18088, 2021.

[24] W. Gong, S. Zhang, Y. Chen et al., "Protective role of hydrogen sulfide against diabetic cardiomyopathy via alleviating necroptosis," *Free Radical Biology and Medicine*, vol. 181, pp. 29–42, 2022.

[25] Y. Zhang, W. Gong, M. Xu et al., "Necroptosis inhibition by hydrogen sulfide alleviated hypoxia-induced cardiac fibroblasts proliferation via sirtuin 3," *International Journal of Molecular Sciences*, vol. 22, no. 21, article 11893, 2021.

[26] S. Yang, M. Xu, G. Meng, and Y. Lu, "SIRT3 deficiency delays diabetic skin wound healing via oxidative stress and necroptosis enhancement," *Journal of Cellular and Molecular Medicine*, vol. 24, no. 8, pp. 4415–4427, 2020.

[27] V. Prabhu, B. S. S. Rao, A. C. K. Rao, K. Prasad, and K. K. Mahato, "Photobiomodulation invigorating collagen deposition, proliferating cell nuclear antigen and Ki67 expression

during dermal wound repair in mice," *Lasers in Medical Science*, vol. 37, no. 1, pp. 171–180, 2022.

[28] S. Song, Y. Ding, G. L. Dai et al., "Sirtuin 3 deficiency exacerbates diabetic cardiomyopathy via necroptosis enhancement and NLRP3 activation," *Acta Pharmacologica Sinica*, vol. 42, no. 2, pp. 230–241, 2021.

[29] B. Wei, H. Zhao, B. Hu et al., "T1AM attenuates the hypoxia/reoxygenation-induced necroptosis of H9C2 cardiomyocytes via RIPK1/RIPK3 pathway," *Biomed Research International*, vol. 2022, Article ID 4833791, 8 pages, 2022.

[30] H. J. Chen, E. E. Ngowi, L. Qian et al., "Role of hydrogen sulfide in the endocrine system," *Frontiers in Endocrinology*, vol. 12, article 704620, 2021.

[31] R. H. Wang, Y. H. Chu, and K. T. Lin, "The hidden role of hydrogen sulfide metabolism in cancer," *Internaitonal Journal of Molecular Sciences*, vol. 22, no. 12, article 6562, 2021.

[32] M. Li, J. Mao, and Y. Zhu, "New therapeutic approaches using hydrogen sulfide donors in inflammation and immune response," *Antioxidants & Redox Signaling*, vol. 35, no. 5, pp. 341–356, 2021.

[33] E. A. Turbat-Herrera, M. J. Kilpatrick, J. Chen et al., "Cystathione β-synthase is increased in thyroid malignancies," *Anticancer Research*, vol. 38, no. 11, pp. 6085–6090, 2018.

[34] Z. Qu, Y. Jiang, B. Q. Wu, Y. F. Duan, Z. D. Sun, and G. H. Luo, "Cystathionine-gamma-lyase inhibitor attenuates acute lung injury induced by acute pancreatitis in rats," *Archives of Medical Science*, vol. 10, no. 4, pp. 825–829, 2014.

[35] W. Guo, D. Li, Y. You et al., "Cystathionine γ-lyase deficiency aggravates obesity-related insulin resistance via FoxO1-dependent hepatic gluconeogenesis," *FASEB Journal*, vol. 33, no. 3, pp. 4212–4224, 2019.

[36] X. Lin, X. Meng, and Z. Song, "Homocysteine and psoriasis," *Bioscience Reports*, vol. 39, no. 11, article 90867, 2019.

[37] A. K. Alshorafa, Q. Guo, F. Zeng et al., "Psoriasis is associated with low serum levels of hydrogen sulfide, a potential anti-inflammatory molecule," *Tohoku Journal of Experimental Medicine*, vol. 228, no. 4, pp. 325–332, 2012.

[38] F. Cai, H. Xu, N. Cao et al., "ADT-OH, a hydrogen sulfide-releasing donor, induces apoptosis and inhibits the development of melanoma in vivo by upregulating FADD," *Cell Death Disease*, vol. 11, no. 1, pp. 1–15, 2020.

[39] F. Cai, H. R. Xu, S. H. Yu et al., "ADT-OH Inhibits Malignant Melanoma Metastasis in Mice Via Suppressing CSE/CBS and FAK/Paxillin Signaling Pathway," *Acta Pharmacologica Sinica*, pp. 1–14, 2021.

[40] J. Lian, G. Ju, X. Cai et al., "Nanofibrous membrane dressings loaded with sodium hydrogen sulfide/endothelial progenitor cells promote wound healing," *Frontiers in Bioengineering and Biotechnology*, vol. 9, article 657549, 2021.

[41] S. C. Kang, E. H. Sohn, and S. R. Lee, "Hydrogen sulfide as a potential alternative for the treatment of myocardial fibrosis," *Oxidative Medicine and Cellular Longevity*, vol. 2020, Article ID 4105382, 14 pages, 2020.

[42] L. Testai, V. Brancaleone, L. Flori, R. Montanaro, and V. Calderone, "Modulation of EndMT by hydrogen sulfide in the prevention of cardiovascular fibrosis," *Antioxidants*, vol. 10, no. 6, article 910, 2021.

[43] Y. Gu, J. Chen, H. Zhang et al., "Hydrogen sulfide attenuates renal fibrosis by inducing TET-dependent DNA demethylation on Klotho promoter," *FASEB Journal*, vol. 34, no. 9, pp. 11474–11487, 2020.

[44] E. J. Macarak, P. J. Wermuth, J. Rosenbloom, and J. Uitto, "Keloid disorder: fibroblast differentiation and gene expression profile in fibrotic skin diseases," *Experimental Dermatology*, vol. 30, no. 1, pp. 132–145, 2021.

[45] D. D. Wu, D. Y. Wang, H. M. Li, J. C. Guo, S. F. Duan, and X. Y. Ji, "Hydrogen sulfide as a novel regulatory factor in liver health and disease," *Oxidative Medicine and Cellular Longevity*, vol. 2019, Article ID 3831713, 16 pages, 2019.

[46] Y. Chen, S. Jin, X. Teng et al., "Hydrogen sulfide attenuates LPS-induced acute kidney injury by inhibiting inflammation and oxidative stress," *Oxidative Medicine and Cellular Longevity*, vol. 2018, Article ID 6717212, 10 pages, 2018.

[47] R. Tabassum and N. Y. Jeong, "Potential for therapeutic use of hydrogen sulfide in oxidative stress-induced neurodegenerative diseases," *International Journal of Medical Sciences*, vol. 16, no. 10, pp. 1386–1396, 2019.

[48] Z. Liu, X. Wang, L. Li, G. Wei, and M. Zhao, "Hydrogen sulfide protects against paraquat-induced acute liver injury in rats by regulating oxidative stress, mitochondrial function, and inflammation," *Oxidative Medicine and Cellular Longevity*, vol. 2020, Article ID 6325378, 16 pages, 2020.

[49] J. Rucker and F. K. Chan, "Tumor-intrinsic and immune modulatory roles of receptor-interacting protein kinases," *Trends in Biochemical Sciences*, vol. 47, no. 4, pp. 342–351, 2022.

[50] X. Liu, X. Xie, Y. Ren et al., "The role of necroptosis in disease and treatment," *MedComm*, vol. 2, no. 4, pp. 730–755, 2021.

[51] M. K. Khoury, K. Gupta, S. R. Franco, and B. Liu, "Necroptosis in the pathophysiology of disease," *American Journal Pathology*, vol. 190, no. 2, pp. 272–285, 2020.

[52] S. Mohammed, E. H. Nicklas, N. Thadathil et al., "Role of necroptosis in chronic hepatic inflammation and fibrosis in a mouse model of increased oxidative stress," *Free Radical Biology and Medicine*, vol. 164, pp. 315–328, 2021.

[53] B. Li, X. Yi, T. Zhuang et al., "RIP1-mediated necroptosis facilitates oxidative stress–induced melanocyte death, offering insight into vitiligo," *Journal of Investigative Dermatology*, vol. 141, no. 12, pp. 2921–2931, 2021.